MOLECULAR AND CELLULAR BIOLOGY, Oct. 2004, p. 8437–8446 Vol. 24, No. 19
0270-7306/04/$08.00+0 DOI: 10.1128/MCB.24.19.8437–8446.2004

Telomere Shortening Exposes Functions for the Mouse Werner and Bloom Syndrome Genes

Xiaobing Du,[1] Johnny Shen,[1] Nishan Kugan,[1] Emma E. Furth,[1] David B. Lombard,[2] Catherine Cheung,[3] Sally Pak,[3] Guangbin Luo,[4] Robert J. Pignolo,[5] Ronald A. DePinho,[6,7] Leonard Guarente,[3] and F. Brad Johnson[1]*

Department of Pathology and Laboratory Medicine[1] and Department of Medicine,[5] University of Pennsylvania School of Medicine, Philadelphia, Pennsylvania; Department of Pathology, Brigham and Women's Hospital,[2] Department of Medical Oncology, Dana-Farber Cancer Institute,[6] and Departments of Medicine and Genetics, Harvard Medical School,[7] Boston, and Department of Biology, Massachusetts Institute of Technology, Cambridge,[3] Massachusetts; and Department of Genetics, Case Western Reserve University, Cleveland, Ohio[4]

Received 28 May 2004/Accepted 18 July 2004

The Werner and Bloom syndromes are caused by loss-of-function mutations in *WRN* and *BLM*, respectively, which encode the RecQ family DNA helicases WRN and BLM, respectively. Persons with Werner syndrome displays premature aging of the skin, vasculature, reproductive system, and bone, and those with Bloom syndrome display more limited features of aging, including premature menopause; both syndromes involve genome instability and increased cancer. The proteins participate in recombinational repair of stalled replication forks or DNA breaks, but the precise functions of the proteins that prevent rapid aging are unknown. Accumulating evidence points to telomeres as targets of WRN and BLM, but the importance in vivo of the proteins in telomere biology has not been tested. We show that *Wrn* and *Blm* mutations each accentuate pathology in later-generation mice lacking the telomerase RNA template *Terc*, including acceleration of phenotypes characteristic of latest-generation *Terc* mutants. Furthermore, pathology not observed in *Terc* mutants but similar to that observed in Werner syndrome and Bloom syndrome, such as bone loss, was observed. The pathology was accompanied by enhanced telomere dysfunction, including end-to-end chromosome fusions and greater loss of telomere repeat DNA compared with *Terc* mutants. These findings indicate that telomere dysfunction may contribute to the pathogenesis of Werner syndrome and Bloom syndrome.

Clues to aging mechanisms have come from segmental progeroid disorders, genetic diseases that hasten certain features of aging. Chief among these is Werner syndrome, characterized by premature aging of the skin, vasculature, and bone and elevated rates of certain cancers, particularly sarcomas (12, 37). A related disease is Bloom syndrome, characterized by limited features of aging, including premature menopause, and by short stature and elevated rates of most cancers (10). Werner syndrome and Bloom syndrome are caused by loss-of-function mutations in *WRN* and *BLM*, respectively, which encode 3′-5′ DNA helicases of the RecQ family (11, 60). The WRN protein also includes a 3′-5′ exonuclease domain not shared with BLM (20, 47). Based on the genome instability in Werner and Bloom syndromes, cell biological studies, biochemical studies of the purified proteins, and genetic studies of RecQ homologues in yeasts and *Escherichia coli*, it is widely accepted that the proteins function in the recombinational repair of stalled replication forks or double-strand breaks (25, 35, 36). Furthermore, there is evidence that WRN and BLM function in S-phase checkpoint and apoptotic responses to DNA damage (25, 35). Several observations indicate that the proteins also play important roles in telomere maintenance (36). Although the maintenance of DNA stability throughout the genome by WRN and BLM presumably contributes substantially to their anticancer activities, it is not yet known what particular functions of the proteins are most important for preventing rapid aging.

Evidence pointing to telomere functions for the WRN and BLM proteins includes the observation that serially passaged Werner syndrome fibroblasts shorten telomeres more rapidly than controls and senesce prematurely (45). Telomere dysfunction likely contributes to the premature senescence because the senescence can be bypassed via artificial expression of telomerase (58). Expression of telomerase also rescues the elevated sensitivity of Werner syndrome cells to certain genotoxic compounds (18), consistent with a possible role for telomere dysfunction in mediating the sensitivity to the compounds. Furthermore, WRN and BLM interact with several proteins critical for telomere function (37), including the TRF2 protein (38), which plays a central role in telomere capping. WRN and BLM occasionally localize to nuclear foci containing telomere DNA (38, 59), particularly in so-called ALT cells that most likely maintain telomeres via recombination (23, 42), and overexpression of BLM lengthens telomeres in ALT cells (49). Additionally, in cells lacking telomerase, the *Saccharomyces cerevisiae* RecQ protein Sgs1p prevents rapid senescence and maintains telomeres via recombination (8, 19, 23).

These observations indicate that WRN and BLM might help maintain telomere integrity, possibly through the repair of damaged telomeres. Consistent with this idea, mouse *Wrn* null mutants are essentially normal and without signs of premature aging (29). The long telomeres and relatively high levels of

* Corresponding author. Mailing address: 405A Stellar Chance Laboratories, 422 Curie Blvd., University of Pennsylvania, Philadelphia, PA 19104-6100. Phone: (215) 573-5037. Fax: (215) 573-6317. E-mail: johnsonb@mail.med.upenn.edu.

telomerase activity in murine cells might mask WRN functions otherwise required to respond to telomere dysfunction. To test this, we asked if shortening of telomeres, via inactivation of the gene encoding the telomerase RNA template component (*Terc*), might expose functions for WRN. Although they possess some unique functions, WRN and BLM appear to have some overlapping activities (22, 25, 36), and so in our experiments we also combined the *Wrn* null mutation with the Blm^{M3} mutation to uncover such functional redundancy. While mice homozygous for *Blm* null alleles die as embryos (7, 14), mice homozygous for the Blm^{M3} hypomorphic mutation develop normally but have elevated rates of cancer after 1 year of age (30, 32). Here we present an analysis of phenotypes that arise in mice with combinations of mutations in the *Wrn, Blm*, and *Terc* loci.

MATERIALS AND METHODS

Mice. $Wrn^{+/-}$ $Blm^{+/-}$ $Terc^{+/-}$ mice were generated by crossing $Wrn^{-/-}$ $Blm^{-/-}$ mice with $Terc^{+/-}$ mice (7, 50). These were in turn crossed to generate $Wrn^{-/-}$ $Blm^{-/-}$ $Terc^{+/-}$ mice, which were crossed with $Wrn^{+/-}$ $Blm^{+/-}$ $Terc^{+/-}$ mice to generate the different G1 mutant lineages. The frequencies of offspring of the different genotypes were at expected Mendelian ratios. Each G1 lineage was crossed to itself to generate G2 lineages, and so forth, using cousin by cousin matings to avoid generation of substrains. All mice were in a mixed genetic background of 50% C57BL/6, 37.5% 129Svj, and 12.5% BALB/c. For the second set of experiments ("new" crosses), mice carrying the three mutations in heterozygous form were crossed for six generations to homogenize the genetic background prior to the generation of G1 lineages. All mice were weighed weekly from weaning at 3 weeks of age until at least 100 days of age. For reasons of space limitation, studies were restricted to mice under 14 months of age. Mice were examined daily, and those judged to be suffering from ill health were sacrificed for analysis. Mouse experimental protocols were approved by the University of Pennsylvania Institutional Animal Care and Use Committee.

Histology and analysis of intestinal crypt apoptosis. Tissues were fixed in 10% formalin overnight at 4°C, followed by storage in 70% ethanol at 4°C; 5-μm sections were stained with hematoxylin and eosin. Quantitation of apoptotic cells and mitoses was performed with the observer blind to genotype, and at least 80 crypts were counted per mouse. For terminal deoxynucleotidyl transferase-mediated dUTP nick end labeling (TUNEL) analyses, 5-μm tissue sections were stained with the ApopTag kit (Intergen) according to the manufacturer's instructions, and at least 50 crypts were counted per mouse.

Bone mineral density measurement. Dual energy X-ray absorptiometry (DEXA) scans were performed of the vertebrae in the abdominal region of anaesthetized mice with a Lunar PIXImus 2. Scans were calibrated with a phantom model with 0.058 g/cm^2 bone mineral density.

Wound healing and hair regrowth assays. After hair removal with electric clippers, full-thickness 3-mm (original crosses) or 4-mm (new crosses) punch biopsies were made through to the panniculus carnosus over each scapula. Two wounds were made per mouse, and five mice per genotype were tested. The long and short axes of each wound were measured daily, and area was calculated with the formula for an ellipse (πab). Hair regrowth assays were done as described (53).

Adult fibroblast culture. Ears were washed for 10 s in 70% ethanol and then in phosphate-buffered saline containing 250 μg of G418 per ml and then minced and digested four times for 30 min in 0.25% trypsin–EDTA at 37°C. Released cells and partially digested tissue were cultured in a 24-well plate in Dulbecco's modified Eagle's medium with 10% heat-inactivated fetal bovine serum, penicillin-streptomycin, 3% O_2, and 5% CO_2 until confluent, and then split into six-well plates. 3T3 proliferation assays were performed in ambient O_2 and 5% CO_2 as described (6). The usual 3-day passage interval was extended in cases where culture growth slowed substantially; in such cases the cells were refed every 3 days and allowed to become nearly confluent before they were passaged.

Cytogenetic analysis and telomere flow fluorescence in situ hybridization. Splenocytes were cultured for 48 h in RPMI with 10% heat-inactivated fetal bovine serum, 10 μg of lipopolysaccharide per ml, and 5 μg of concanavalin A per ml and then arrested for 30 min with 0.75 μg of colcemid per ml. Metaphases were fixed, stained with 4′,6′-diamidino-2-phenylindole (DAPI), and analyzed as described (44). For samples from the new crosses, metaphases were scored by an observer blind to genotype. For telomere signal-free end analyses, metaphase spreads were stained with DAPI and a indocarbocyanine-conjugated peptide nucleic acid (PNA) telomere repeat probe, indocarbocyanine-OO-$(CCCTAA)_3$ (Boston Probes) as described (Unit 18.4, Current Protocols in Cell Biology Online, 2003 [www.interscience.wiley.com]). Telomere flow fluorescence in situ hybridization was performed on bone marrow cells with a fluorescein isothiocyanate-labeled PNA telomere repeat probe as described (2). Telomere fluorescence per cell was calculated for cells gated in the G_1 phase of the cell cycle based on DNA content, and telomere fluorescence for each sample was corrected for background fluorescence by control hybridizations of the same sample without the telomere PNA probe. All samples to be compared directly were processed and measured by flow cytometry on the same days to avoid interrun variability. Repeat measurements of the same sample yielded a coefficient of variation of 6%.

Statistical tests. Graphpad Prism 3 software was used for statistical analyses. Unpaired two-tailed *t* tests were used to compare each genotypic group for the data in Fig. 1 to 4 and 6. Kaplan-Meier analyses were performed for the data in Fig. 5, and significance was determined with a log-rank test. Error bars in all figures indicate the standard error of the mean.

RESULTS

Generation of mice with mutations in *Wrn*, *Blm*, and *Terc* and characterization of fertility defects. Earlier work had demonstrated that mice doubly homozygous for the Blm^{M3} hypomorphic allele and a *Wrn* null allele were viable and fertile (28, 50). Such $Wrn^{-/-}$ $Blm^{M3/M3}$ mice were crossed with $Terc^{+/-}$ mice to generate $Wrn^{+/-}$ $Blm^{+/M3}$ $Terc^{+/-}$ triple heterozygotes, which were in turn crossed to generate four lineages: wild type, $Wrn^{-/-}$ $Blm^{M3/M3}$ (wb), $Terc^{-/-}$ (t), and $Wrn^{-/-}$ $Blm^{M3/M3}$ $Terc^{-/-}$ (wbt) (see Materials and Methods). $Terc^{-/-}$ mice must be bred for several generations before telomeres become sufficiently short to elicit pathology (44), and so we carried each lineage through multiple generations.

The first and second generations (G1 and G2) of each lineage were fertile, and no abnormalities were observed for the first year of life in general appearance, body weight, or histologic surveys of the following organs: thymus, lymph nodes, spleen, heart, lung, gastrointestinal tract, liver, pancreas, submandibular gland, kidney, adrenal gland, skeletal muscle, bone marrow, femur, vertebrae, skin, ovaries, and testes (not shown). However, a decline in fertility was evident in G3 wbt mutants, and G4 wbt mutants were sterile; in contrast, the wb and t lineages each generated viable offspring through G7 (Fig. 1A). Gross and histological examination of gonads from G4 triple mutant mice revealed marked atrophy. In males, this was characterized by a decline in testes mass (Fig. 1B) and by the loss in seminiferous tubules of spermatogenic cells and mature sperm (Fig. 1C). These findings are similar to those observed in later-generation $Terc^{-/-}$ mutants (17, 26, 44) (Fig. 1B, G6 t mice) but occur approximately two to three generations earlier in wbt mutants.

Although the differences in fertility between the t and wbt mice were large, it was possible that the mixed genetic background of the mice or differences in telomere length among the founders of each lineage might have contributed in a random fashion to the phenotypic differences. To control for these possibilities, we repeated the experiment; hereafter we refer to the first set of crosses as original crosses and the repeat set of crosses as new crosses. Furthermore, prior to beginning the new crosses, we first homogenized the genetic background of the mice through six generations of parent-offspring and intersibling crosses of mice carrying the three mutations in heterozygous form. In addition, in the new crosses, $Wrn^{-/-}$ (w),

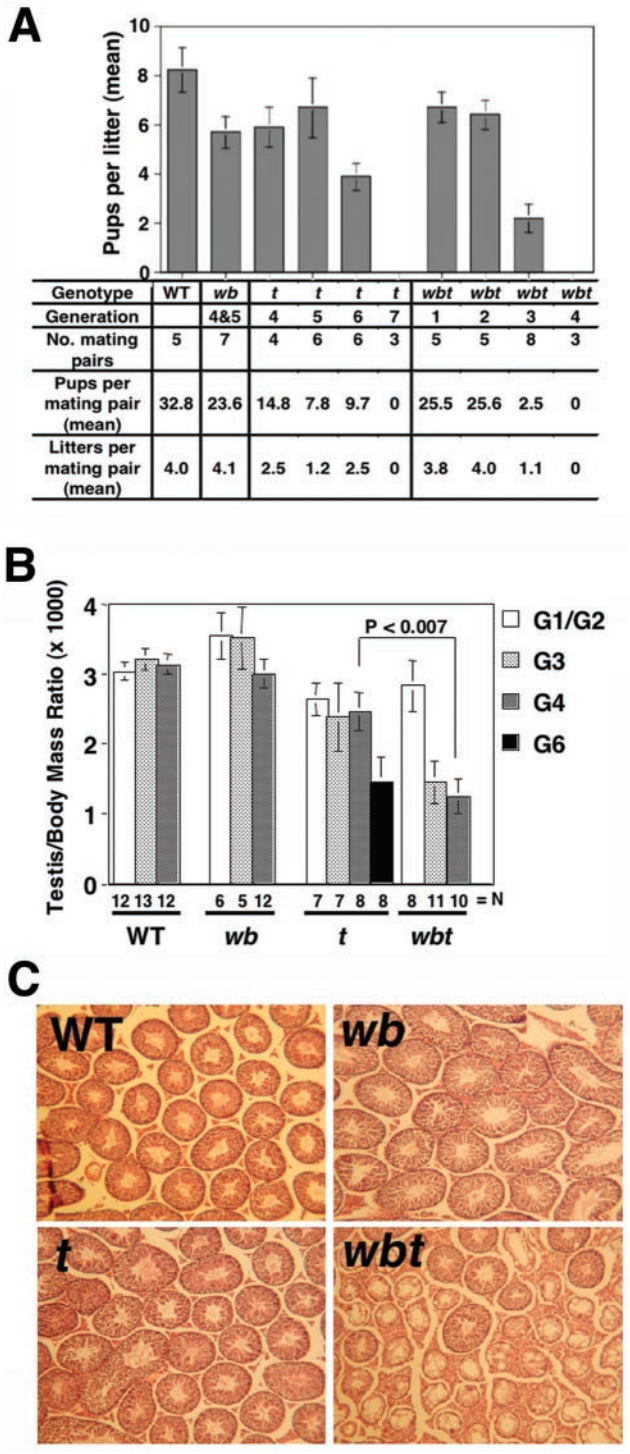

Genotype	WT	*wb*	*t*	*t*	*t*	*t*	*wbt*	*wbt*	*wbt*	*wbt*
Generation		4&5	4	5	6	7	1	2	3	4
No. mating pairs	5	7	4	6	6	3	5	5	8	3
Pups per mating pair (mean)	32.8	23.6	14.8	7.8	9.7	0	25.5	25.6	2.5	0
Litters per mating pair (mean)	4.0	4.1	2.5	1.2	2.5	0	3.8	4.0	1.1	0

FIG. 1. Reproductive defects in mice with combination of mutations in *Wrn, Blm*, and *Terc*. (A) Indices of fertility for the first four months of mating. The mean number of pups in each litter for the indicated genotypes and generation are graphed with standard errors. Also indicated are the numbers of mating pairs and mean numbers of pups and litters generated per mating pair. WT, wb, t, and wbt indicate wild-type, $Wrn^{-/-}$ $Blm^{M3/M3}$, $Terc^{-/-}$, and $Wrn^{-/-}$ $Blm^{M3/M3}$ $Terc^{-/-}$ genotypes, respectively. Data from G4 and G5 wb mutants were not significantly different and were pooled. (B) Testes-to-body mass ratios (multiplied by 1,000) for mice of the indicated genotypes and generations. Data for G1 and G2 mice were not significantly different and were pooled. The number of mice examined is indicated (*N*). Within each generation, mice were of the same mean age, which was 10, 7.5, 6, and 6 months for G1/G2, G3, G4, and G6, respectively. (C) Representative histologic sections of testes from G4 mice of the indicated genotypes. G4 wbt testes have smaller seminiferous tubule cross sections, absence of spermatogenesis in most tubules, and an apparent increase in Leydig cells surrounding the tubules. All data are for mice from the original crosses.

$Blm^{M3/M3}$ (b), $Wrn^{-/-}$ $Terc^{-/-}$ (wt), and $Blm^{M3/M3}$ $Terc^{-/-}$ (bt) lineages were also generated to gauge the individual contributions of *Wrn* and *Blm* mutations to the phenotypes. Consistent with results from the original crosses, wbt mice from the new crosses became infertile rapidly, at G3 (one generation earlier than they had in the original crosses), while the other genotypes were fertile through at least G4 (data not shown). Moreover, for the original four genotypes (wild type, wb, t, and wbt), all of the phenotypes tested in both the original and new crosses (fertility, body weight, intestinal pathology, wound healing, and cytogenetics; see below) were affected consistently, indicating that the differences observed between lineages are a consequence of their different *Wrn*, *Blm*, and *Terc* genotypes.

Body mass and habitus and bone density. wbt triple mutants, like the other genotypes, had normal body weight in G1 (data not shown), but G3 and G4 wbt mutants weighed less and were smaller than controls. Weekly measurements revealed differences in the body mass apparent at 3 weeks of age and which increased as the mice grew older (Fig. 2A and 2B). G3 bt mutants also weighed less than controls, but not as little as G3 wbt mutants, indicating that the *Blm* and *Wrn* mutations each contribute to low body weight in wbt mutants (Fig. 2C).

G3 and G4 wbt mutants frequently developed a kyphotic (hunched) and scruffy appearance (Fig. 2A). Consistent with the observed kyphosis, DEXA (dual energy X-ray absorptiometry) scans of G3 mice revealed reduced bone density in the vertebral skeleton of wbt mutants compared with controls (Fig. 2D). Although increased hair loss was sometimes observed in aging G3 and G4 wbt mutants, hair regrowth assays did not reveal significant differences between the different mutant lineages (data not shown).

Gastrointestinal pathology of mutant mice. We noticed that G3 and G4 wbt and bt mutant mice suffered from chronic diarrhea and frequently developed prolapse of the rectum (Fig. 2A). At the histological level, the appearance of the small intestines of all G1 genotypes was normal, but compared with controls, the small intestines of G3 and G4 wbt mice were characterized by distortion of crypt architecture and signs of acute inflammation, including blood vessel dilatation and neutrophil infiltration (Fig. 3A). Under normal conditions, intestinal epithelial cells undergo apoptosis at the end of their developmental cycle as they are sloughed off the tips of villi, but in contrast, epithelial cells in the crypts do not normally undergo apoptosis. However, crypt cells do apoptose in late-generation telomerase mutants (17, 44).

To test if *Wrn* and *Blm* mutation influenced the level of crypt apoptosis associated with *Terc* mutation, we quantified apoptosis by direct histologic examination of hematoxylin- and eosin-stained tissue sections and confirmed these data by quantifying TUNEL-positive nuclei in the tissue sections (Fig. 3B).

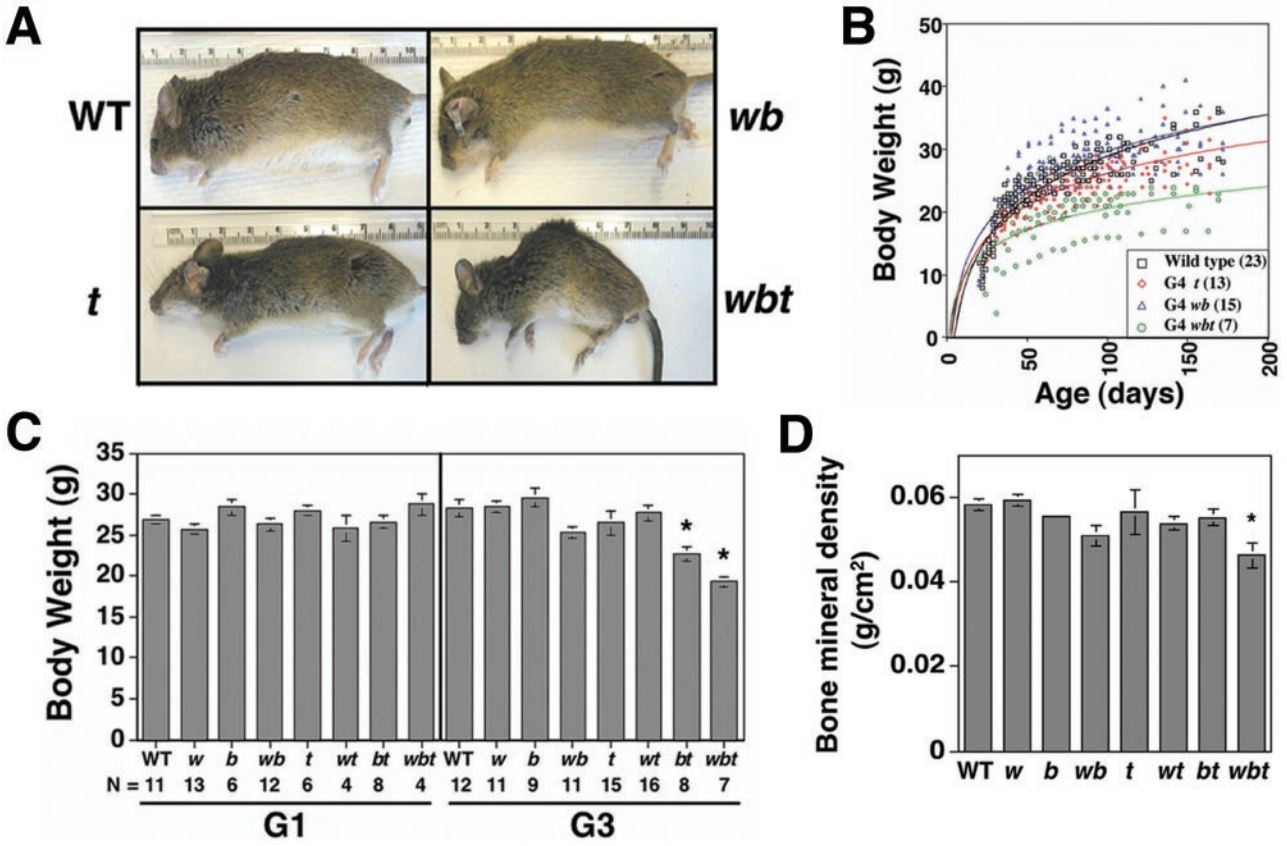

FIG. 2. Body habitus, mass, and bone density of the mutant mice. (A) Representative 8-month-old G4 males of the indicated genotypes (original crosses) were photographed after anesthesia. Note small size, kyphosis, and rectal prolapse in the wbt mutant. Genotype abbreviations are the same as for Fig. 1. (B) Growth curves for G4 male mice from 3 weeks through 5 months of age. Weekly body weights are plotted versus age for G4 mice of the indicated genotypes (original crosses), and fitted logarithmic curves are shown. The numbers of mice of each genotype are indicated in parentheses. Note that although two wb mice were heavier than the wild-type controls, the mean masses of wb mice were not significantly different from that of wild-type mice. (C) Body weights at 80 days of age for G1 and G3 male mice of the indicated genotypes (new crosses). For each mouse, the weight at 80 days was averaged with those from 1 week earlier and 1 week later. *N* is the number of mice in each group, mean values and standard errors are shown, and * indicates $P < 0.05$ in comparison with each other G3 genotype. Genotype abbreviations are the same as for Fig. 1, and in addition w, b, wt, and bt indicate $Wrn^{-/-}$, $Blm^{M3/M3}$, $Wrn^{-/-}$ $Terc^{-/-}$ and $Blm^{M3/M3}$ $Terc^{-/-}$ genotypes, respectively. (D) Vertebral bone mineral density from DEXA scans of 4.5-month-old G3 females of the indicated genotypes (five mice per genotype). Mean values and standard errors are shown, and * indicates $P < 0.05$ compared with t mice.

Levels of apoptosis in intestinal crypts were slightly elevated in G3 t and wt mutants but markedly elevated in G3 and G4 wbt mice compared with controls and reached the levels observed in G7 t mutants (Fig. 3B). G3 bt mutants had levels of apoptosis as high as that of G3 wbt mutants, while G3 wt mutants had levels similar to that of G3 t mutants, indicating that, in this particular tissue, *Blm* may have a greater role than *Wrn* in the context of telomerase inactivation. Furthermore, we confirmed through TUNEL analysis that levels of apoptosis in G1 wbt mutants were not elevated (Fig. 3B), indicating that this phenotype depends on telomere loss and not loss of telomerase per se.

Wound healing and skin fibroblast proliferation. Individuals with Werner syndrome suffer from chronic skin ulcers, particularly around the ankles, and late-generation *Terc* mutants display slow wound healing (12, 44). We therefore tested our mice for rates of wound healing and observed slow wound healing in G3 wbt mutants compared with controls (new crosses; Fig. 4A). Although the *Wrn* and *Blm* mutations each contributed to the slow healing of wbt mutants, the *Wrn* mutation appeared to contribute more than the *Blm* mutation because G3 wt but not G3 bt mutants healed wounds more slowly than the controls. Wound healing involves the interplay of several cell types, and we do not yet understand the basis for this defect. However, one cell type important for wound healing is the dermal fibroblast, and we observed significant growth defects in cultured adult skin fibroblasts from wbt mutants compared with controls (Fig. 4B).

Skin fibroblasts were obtained from the ears of 10-month-old G1 siblings (new crosses) and cultured serially in 3T3 assays. No significant differences in the rates of culture doubling were observed between wild-type and t cells, consistent with earlier studies (6), while wb and wbt cultures doubled more slowly but similarly to each other in early passages. However, after seven population doublings, the wbt cells slowed and failed to proliferate further for over 1 month. Based on the sloughing of cells that failed to exclude trypan blue from the plate into the medium and based on the enlarged and flattened

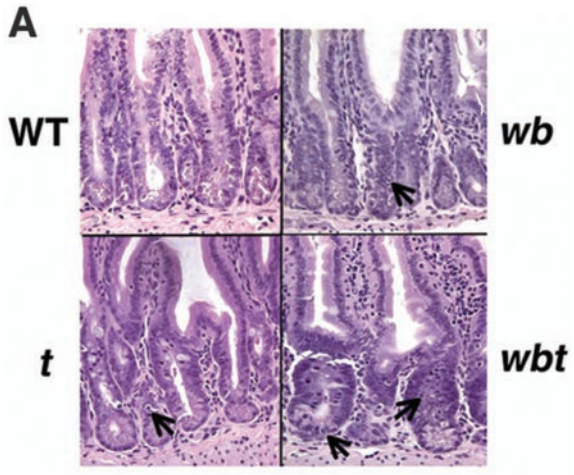

B

Genotype	H&E Analyses		TUNEL Analyses	
	Apoptoses/crypt	P value	Apoptoses/crypt	P value
WT	0.016 +/- 0.007		0.066 +/- 0.046	
w	0.021 +/- 0.008		0.062 +/- 0.014	
b	0.051 +/- 0.022		0.071 +/- 0.051	
wb	0.025 +/- 0.017		0.037 +/- 0.002	
t	0.379 +/- 0.139		0.405 +/- 0.162	
wt	0.206 +/- 0.041		0.427 +/- 0.232	
bt	1.58 +/- 0.404	0.001	2.07 +/- 0.228	0.004
wbt	1.33 +/- 0.250	< 0.001	2.89 +/- 0.399	0.005
G1 *wbt*	ND		0.072 +/- 0.021	
G7 *t*	1.11 +/- 0.130	< 0.001	2.40 +/- 0.171	0.001

FIG. 3. Small intestine pathology in mutant mice. (A) Representative histologic sections of G4 small intestines from 8-month-old mice of the indicated genotypes stained with hematoxylin and eosin (original crosses). Representative apoptotic nuclei are indicated by arrows. (B) Frequency of apoptotic cells in small intestine crypts (new crosses) assessed by examination of nuclear morphology in hematoxylin- and eosin-stained histologic sections (H&E) and by TUNEL staining of histologic sections. All genotypes are for G3 mice except for G1 wbt and G7 t mice, as indicated. Apoptotic nuclei were counted in at least 80 crypts for hematoxylin and eosin and 50 crypts for TUNEL analysis per mouse, and the mean number of apoptotic cells per crypt and standard errors are shown. For hematoxylin and eosin analyses, four female mice (4.5 months old) were analyzed per genotype except for three mice for G7 t, and for TUNEL analyses three mice were analyzed per genotype. *P* values for pairwise comparisons with all other genotypes are shown. There were no significant differences in the number of mitoses per crypt among the different genotypes (data not shown).

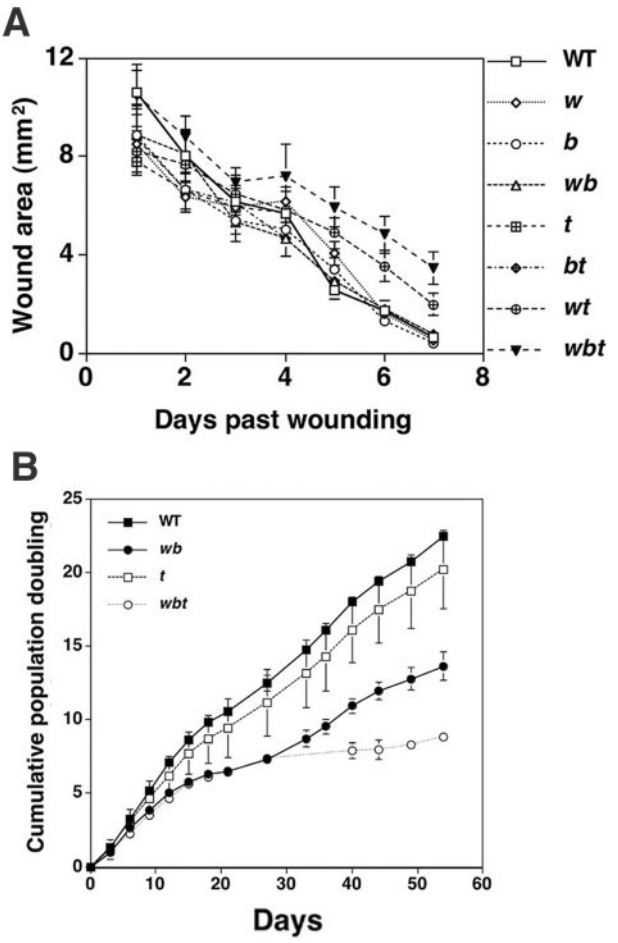

FIG. 4. Wound healing and dermal fibroblast growth. (A) Wound healing in G3 females (five mice per genotype, new crosses). Two full-thickness 4-mm punch biopsy wounds were made for each mouse in skin overlying the scapulae, and wound areas were measured for the next 7 days. Mean values and standard errors are shown. Compared with all faster-healing genotypes, wt is different at $P < 0.05$ at day 6, and wbt is different at $P < 0.01$ at days 6 and 7. Similar results were obtained for mice from the original crosses (data not shown). (B) Culture growth of skin fibroblasts. Fibroblasts cultured from the ears of two G1 siblings per genotype (new crosses) were passaged serially, and cumulative doublings were measured. Mean values and standard errors are indicated.

appearance of the remaining adherent cells, a mixture of cell death and senescence might be responsible for the poor growth of the triple mutant cultures. It is possible that the impaired growth of wbt cells from G1 mice after serial culture under the damaging conditions of standard cell culture (41) reflects defects that also occur at later generations in vivo in wbt mice. Regardless, these observations provide another example of how mutations in *Wrn*, *Blm*, and *Terc* synergize to affect cell function.

Reduced life span of later-generation wbt mice. Consistent with their frail appearance, we observed a dramatically reduced life span in G3 wbt mutants versus controls. As shown in Fig. 5, the median age of death for G3 wbt mutants was 7 months, compared with greater than 10 months for all other genotypes ($P < 0.0001$ compared with all other genotypes by log-rank test). In addition, G3 bt mice also have a significantly reduced life span, with a median age of death of 11 months ($P \leq 0.002$ compared with all other genotypes by log-rank test). Because the G3 wbt life span is significantly shorter than the G3 bt life span, the *Wrn* mutation contributes to the mortality of the wbt mutants, even though it has no effect on life span in the presence of active telomerase and also does not appear to shorten life span dramatically in G3 wt mice (Fig. 5) (28). There was no increased mortality for any of the genotypes in G1 animals during the first year of life (data not shown), indicating that the rapid mortality of G3 wbt and bt mutants apparently depends on telomere shortening.

Telomere function and length. The pathology observed in wbt mutants could arise from direct exacerbation by *Wrn* and *Blm* mutation of telomere dysfunction initiated by loss of telomerase, or it might instead reflect the summation of genome-

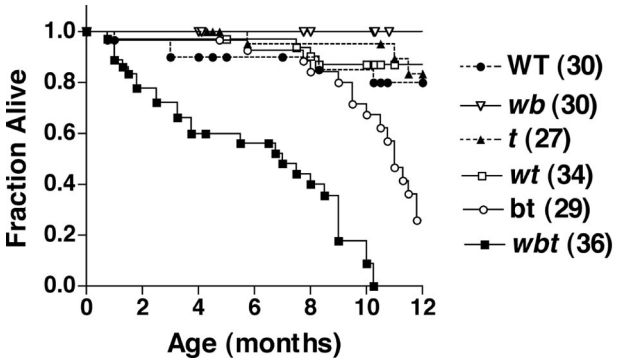

FIG. 5. Shortened life spans of G3 wbt and bt mice. Kaplan-Meier analysis of survival in G3 wild-type, wb, t, wt, bt, and wbt mice (new crosses) is shown. w and b single mutants had no shortening of life span for the 12 months examined, and they were omitted for clarity. Only natural deaths were counted in the analyses; data for mice harvested for analytical autopsy were censored in the analysis and are indicated as points on each line that are not associated with a drop in the fraction alive. The numbers of mice in each cohort are indicated in parentheses. By log-rank test, the G3 wbt life span was shorter than that of all other genotypes at $P < 0.0001$, and G3 bt life span was different from all other genotypes at $P \leq 0.002$.

wide instability caused by mutation of *Wrn* and *Blm* combined with genome instability caused by loss of telomerase. To begin to address these possibilities, we tested aspects of telomere function. A cardinal indicator of telomere dysfunction is end-to-end chromosomal fusion, which becomes more frequent in later-generation $Terc^{-/-}$ mice (15). Fusion levels in metaphase spreads from splenocytes from G1 mice were not elevated for any genotype, but were significantly elevated in G3 and G4 wbt mutants (Fig. 6A and 6C). Neither G3 bt nor wt mutants had significant elevations in fusions, indicating that the *Wrn* and *Blm* mutations each contribute to this wbt phenotype.

Telomere dysfunction in wbt triple mutants could reflect a propensity of telomeres, at a given degree of shortening, to malfunction in the absence of WRN and BLM or could reflect an elevated loss of telomere repeat DNA in wbt compared with $Terc^{-/-}$ mutants or both. Flow fluorescence in situ hybridization analysis of bone marrow cells indicated no differences in telomere length among G1 genotypes but revealed a significantly shorter mean cellular telomere length in G3 and G4 wbt samples compared with t samples (Fig. 6B). Consistent with these measurements, the frequency of chromatid termini without detectable telomere repeat DNA in metaphase chromosome spreads (signal-free ends) was elevated in samples from G3 wbt compared with G3 t samples (Fig. 6C and 6D). Therefore, at least one contributor to the severe phenotypes of late-generation wbt mutants appears to be accentuated loss of telomere repeat DNA in this lineage compared with the t lineage. Furthermore, the occurrence of signal-free ends was not increased in wb mutants, indicating that, at least in the presence of telomerase, the *Wrn* and *Blm* mutations do not themselves cause significant telomere repeat loss. This contrasts with a recent demonstration of stochastic loss of complete telomere repeat arrays at chromosome ends in a telomerase-positive human tumor cell line overexpressing a dominant-negative form of *WRN* (3) and suggests that, in murine splenocytes, the *Wrn* and *Blm* mutations either do not cause such complete loss events or that telomerase is sufficient to repair such events.

DISCUSSION

To address the possibility that the WRN and BLM proteins have important functions in the setting of telomere dysfunction, we tested the phenotypic consequences of *Wrn* and *Blm* mutations in mice with telomeres that had been shortened artificially via mutation of the *Terc* RNA component of telomerase. We found that the *Wrn* and *Blm* mutations each contributed to the acceleration, by two to three generations, of several phenotypes characteristic of later-generation *Terc* mutants, including infertility, apoptosis of intestinal crypt epithelial cells, impaired wound healing, and chromosome end-to-end fusions. These findings are consistent with the accentuated telomere repeat loss observed in the wbt triple mutants compared with $Terc^{-/-}$ single mutants. However, other phenotypes, including reduced body mass at early ages and reduced bone density, have not been observed in $Terc^{-/-}$ mice and so may reflect the recreation in the mouse of pathology seen in Werner or Bloom syndrome: low bone density is found in Werner syndrome, and reduced body mass is found in Bloom syndrome and to a lesser degree in Werner syndrome (10, 12). Consistent with this view, the *Blm* mutation contributed more than the *Wrn* mutation to the low body weight of wbt mice. Furthermore, some wbt phenotypes are characteristic of both the human syndromes and late-generation $Terc^{-/-}$ mice, including fertility defects in Werner syndrome and Bloom syndrome, and chronic wounds in Werner syndrome, and so it is unclear if they reflect a simple acceleration of $Terc^{-/-}$ phenotypes or additional interactions between shortened telomeres and the *Wrn* and *Blm* mutations.

An important aspect of wbt phenotypes is that several reflect synergistic genetic interactions among the *Wrn*, *Blm*, and telomerase mutations: the defects, including those in fertility and testes mass, intestinal apoptosis, chromosome fusion, rates of wound healing, and growth of fibroblast cultures, are more severe in the triple mutants than the sum of these defects in each single mutant. Thus, the mutations are not acting independently, but the three genes function together, possibly through direct action of the WRN and BLM proteins at telomeres. Because G1 mutants were unaffected, the effects of *Wrn* and *Blm* mutation in wbt mutants are not caused by loss of telomerase activity per se, but apparently require telomere shortening. Faster loss of telomere repeat DNA and higher levels of chromosome end-to-end fusions in wbt mutants suggest that WRN and BLM might have direct effects at telomeres. Alternatively, telomere dysfunction may synergize with nontelomeric defects caused by *Wrn* and *Blm* mutation: DNA damage signals from shortened telomeres might add to damage signals throughout the genome to exceed a threshold that signals cell death or growth arrest, or a reduction in DNA repair capacity caused by telomere dysfunction (55a) might synergize with DNA repair defects caused by Wrn and Blm mutation. Both models may be correct, and the interaction of WRN and BLM with TRF2 and other telomere maintenance proteins, including Ku and DNA-PKcs (37), supports the first idea, while the phenotypes observed in wbt but not $Terc^{-/-}$ mice support the second.

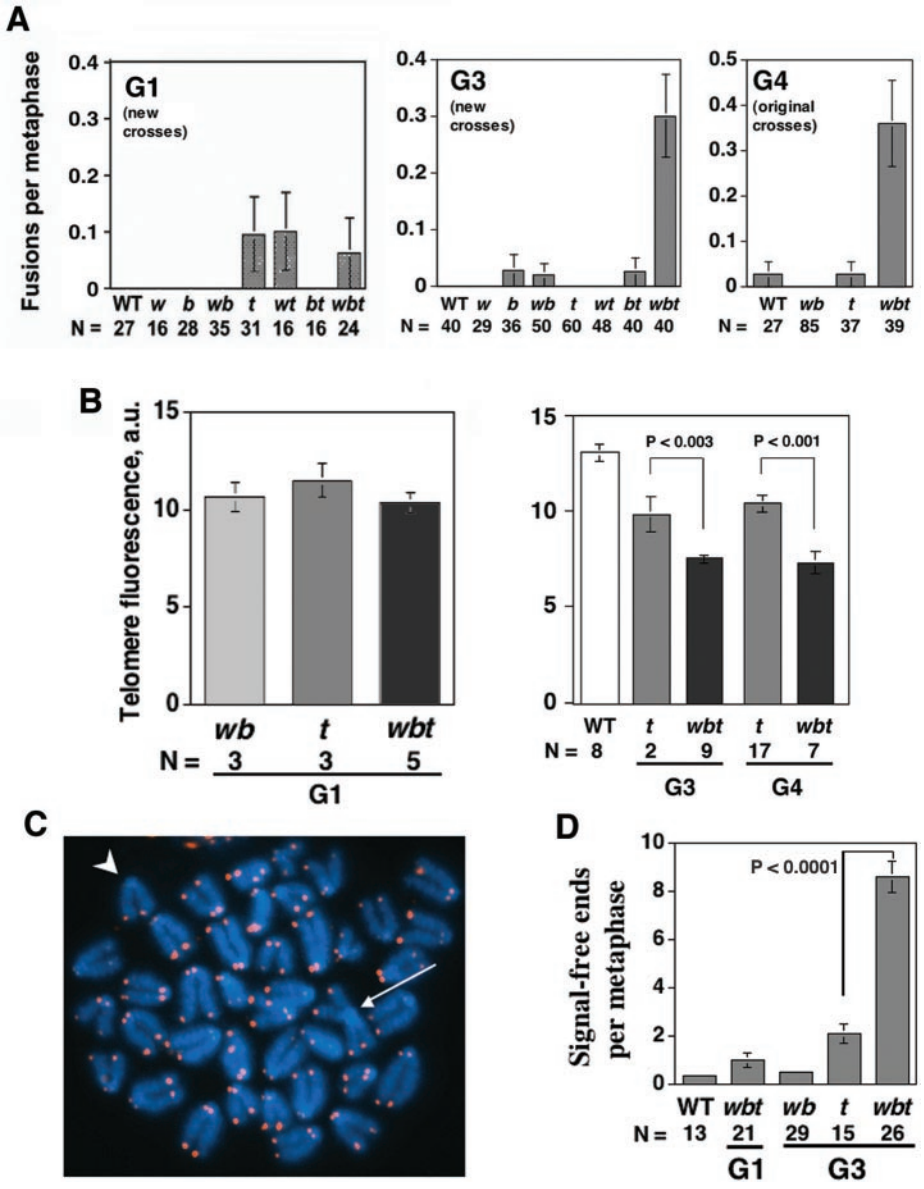

FIG. 6. Cytogenetic and telomere length analyses. (A) Frequency of chromosome end-to-end fusions (p-to-p and q-to-q) in cultured splenocytes from G1 and G3 mice (new crosses) and G4 mice (original crosses) of the indicated genotypes. *N* is the number of metaphases analyzed. For original crosses, mice were 7 to 10 months old; for new crosses, mice were 4.5-month-old females, four to six mice per genotype. Means and standard errors are shown. (B) Telomere length of G1 wb, t, and wbt mice (left) and wild-type and G3 and G4 t and wbt mice (right), measured by flow fluorescence in situ hybridization of bone marrow cells (original crosses). The mean ages of the G1 wb, t, and wbt, wild-type, G3 t and wbt, and G4 t and wbt mice were 11, 12, 10, 10, 14, 14, 9, and 7 months, respectively. Means, standard errors, and *P* values are indicated. The older age of the G3 mice likely explains why their telomeres are not significantly longer than that of the G4 mice. Measurements of the group on the left were performed on a different day than those of the group on the right, and so the values are not directly comparable between the groups. (C) Representative splenocyte metaphase from a G3 wbt mutant stained for DNA with DAPI (blue) and telomeric repeat DNA with an indocarbocyanine-labeled PNA telomere repeat probe (red). The arrowhead indicates a representative signal-free end, and the arrow indicates a p-to-p chromosome end fusion that lacks telomeric DNA at the fusion point. (D) Quantitation of signal-free ends on splenocyte metaphase chromosomes from mice of the indicated genotypes (new crosses). Chromosomes were stained as in C. *N* is the number of metaphases analyzed, and mean values, standard errors, and the *P* value for wbt versus t are shown.

The first idea is also supported by studies from our laboratory investigating how mutation of the *SGS1* RecQ family helicase of *S. cerevisiae* accelerates the rate of senescence of yeast telomerase (*tlc1*) mutants. We have found that null mutations in a variety of loci required for normal DNA replication, repair, and recombination, including *TOP1*, *MUS81*, *SLX4*, *RRM3*, and *SRS2*, have no effect on the rate of senescence of *tlc1* mutants (M. Azam, J. Y. Lee, and F. B. Johnson, unpublished results), consistent with published findings that mutations in *RAD1*, *RAD10*, and *POL3* also do not affect the rate of senescence of telomerase mutants (43). Thus, accelerated senescence in *sgs1 tlc1* mutants is unlikely to be a conse-

quence of generic genome instability but rather reflect a specific function of the Sgs1 protein, perhaps at telomeres. Regardless of the precise mechanisms by which the *Wrn*, *Blm*, and *Terc* mutations interact, our findings indicate that the *Wrn* and *Blm* mutations can accentuate the pathology associated with telomere shortening, a process associated with natural human aging, and thus indicate that the pathology of Werner and Bloom syndromes may involve telomere dysfunction.

How might telomere defects contribute to premature aging in Werner syndrome? Werner syndrome aging pathology occurs principally in mesodermal tissues, such as bone, dermis, and vascular endothelium, which normally have slow rates of cell turnover and low levels of telomerase activity (13). In contrast, highly proliferative tissues, such as the hematopoietic system and gastrointestinal tract, which have relatively high levels of telomerase, and the central nervous system, which is effectively postmitotic and does not shorten telomeres with age (2), are relatively spared premature aging. Given the data presented here and elsewhere indicating that telomerase compensates for some defects caused by loss of RecQ family proteins (8, 19, 23), the distribution of defects in Werner syndrome could indicate tissues where cell turnover rates are high enough to cause telomere shortening with age but telomerase activity is too low to prevent telomere dysfunction. In contrast, $Terc^{-/-}$ mice have no telomerase activity in any tissue, and so tissues with the highest rate of cell turnover, and thus presumably the fastest telomere shortening, are most affected by combined mutations in *Terc*, *Wrn* and *Blm*. This explains why wbt mice but not humans with Werner and Bloom syndrome develop degenerative pathology in the small intestine: humans with these diseases are presumably replete with telomerase in this organ, protecting them from telomere defects.

This may also explain why premature aging is less pronounced in Bloom syndrome than Werner syndrome, because unlike WRN, which is expressed broadly in many tissues, BLM is preferentially expressed in highly proliferative tissues, including the male germ line and thymic lymphocytes (24, 60). These tissues express substantial levels of telomerase and so may be relatively protected from telomere dysfunction (27, 57). This model cannot fully explain the fertility defects in Werner syndrome and Bloom syndrome, because germ cells express high levels of telomerase, but it is likely that meiotic functions of WRN and BLM contribute to normal fertility (33, 55). Furthermore, cancer can arise in both Werner syndrome and Bloom syndrome in tissues with high levels of telomerase, for example, in the hematopoietic system, but this may reflect principally the widespread genome instability characteristic of these diseases rather than a telomere-specific defect.

If WRN and BLM indeed play direct roles at telomeres, by what mechanisms might they maintain telomere function? First, WRN and BLM might play a role in the recombinational repair of telomeres. This is supported by the high levels of WRN and BLM protein in foci containing telomeric DNA in ALT cells (23, 59), which most likely use recombinational mechanisms to maintain their telomeres (42), by the ability of overexpressed BLM to lengthen telomeres in ALT cells (49), and by the requirement for yeast Sgs1p for the generation of type II survivors of telomerase deletion, which use recombination to maintain telomeres (8, 19, 23). The recent finding that downregulation of *RAD51D* expression causes telomere shortening and dysfunction in primary murine cells is consistent with a role for recombination in the normal maintenance of telomeres (52).

Second, WRN and BLM could regulate T-loop assembly or disassembly. WRN and BLM interact functionally with TRF2, which catalyzes T-loop formation in vitro (37, 48), and thus might modulate the ability of TRF2 to regulate T-loop assembly. T-loops include a D-loop at their base, and WRN helicase and exonuclease activities catalyze the disassembly of D-loops in vitro (38), and further, the degradation of synthetic T-loops by the WRN exonuclease was recently shown to be stimulated by TRF2 in vitro (31). Third, WRN and BLM may participate in the replication or processing of telomere ends. FEN-1 (flap endonuclease 1), which is required for proper Okazaki fragment processing during lagging-strand DNA synthesis, is strongly stimulated in vitro by purified WRN and BLM (46) and may thus cooperate with WRN and BLM in telomere replication. Together, the proteins might be particularly important for telomere lagging-strand synthesis because of the absence of a "backup" 3′ end at the telomere terminus from which repair synthesis to replace defective Okazaki fragments might otherwise be primed (39). Consistent with this possibility, *S. cerevisiae* cells with a mutation of the FEN-1 ortholog *RAD27* incur high levels of single-stranded DNA principally at telomere ends (39), and shorten their telomeres more rapidly in the setting of genetic inactivation of telomerase (40). Fourth, G quadruplexes, which form at telomeric DNA in vitro and are favored substrates of RecQ helicases (21), might accumulate at shortening telomeres and require WRN or BLM to unwind them. One or more of these mechanisms may be operative, and our mouse models provide useful materials to further determine how WRN and BLM may participate in telomere maintenance.

Finally, we note that although it is clear that human aging is accompanied by telomere shortening in several tissues, it remains uncertain if telomere dysfunction plays a causal role in aging (4, 54). While telomere shortening is one contributor to telomere dysfunction and telomere dysfunction can in turn cause apoptosis or senescence in cultured cells (5), whether telomeres ever become critically short in aged humans remains undetermined. The remarkable similarities between the Werner syndrome phenotype and certain features of natural aging, in combination with our findings and those of others that indicate a role for WRN in the setting of telomere dysfunction, provide circumstantial support for the hypothesis that telomeres may play an important role in the aging process, and the tissues affected by premature aging in Werner syndrome might point to those that are most susceptible to telomere dysfunction during natural aging. Furthermore, because telomere dysfunction contributes to overall genome instability and is itself interpreted by the cell as a form of DNA damage (9, 51), our findings are consistent with the many observations indicating a role for genome maintenance in the promotion of longevity (16, 56).

ACKNOWLEDGMENTS

We thank the Center for Neurological and Degenerative Disease Research and the Center for Molecular Studies in Digestive and Liver Disease for histology assistance, the Mouse Phenotyping, Physiology and Metabolism Core for DEXA scans, J. Martin for database assis-

tance, S. Chang for communication of unpublished findings, and R. A. Marciniak and members of the Johnson lab for helpful discussions.

This work was supported by R03 and R55 awards from the NIA and a Paul Beeson Award from AFAR (F.B.J.) and by grants from the NIH, Ellison Medical Foundation, and the Howard and Linda Stern Fund (L.G.).

ADDENDUM IN PROOF

Findings consistent with ours, that Wrn and Terc mutations cause synergistic phenotypes in late-generation mice, have been reported recently by S. Chang et al. (Nat. Genet. **36:**877–882, 2004).

REFERENCES

1. **Allsopp, R. C., E. Chang, M. Kashefi-Aazam, E. I. Rogaev, M. A. Piatyszek, J. W. Shay, and C. B. Harley.** 1995. Telomere shortening is associated with cell division in vitro and in vivo. Exp. Cell Res. **220:**194–200.
2. **Baerlocher, G. M., J. Mak, T. Tien, and P. M. Lansdorp.** 2002. Telomere length measurement by fluorescence in situ hybridization and flow cytometry: tips and pitfalls. Cytometry **47:**89–99.
3. **Bai, Y., and J. P. Murnane.** 2003. Telomere instability in a human tumor cell line expressing a dominant-negative WRN protein. Hum. Genet. **113:**337–347.
4. **Ben-Porath, I., and R. A. Weinberg.** 2004. When cells get stressed: an integrative view of cellular senescence. J. Clin. Investig. **113:**8–13.
5. **Blackburn, E. H.** 2001. Switching and signaling at the telomere. Cell **106:** 661–673.
6. **Blasco, M. A., H. W. Lee, M. P. Hande, E. Samper, P. M. Lansdorp, R. A. DePinho, and C. W. Greider.** 1997. Telomere shortening and tumor formation by mouse cells lacking telomerase RNA. Cell **91**:25–34.
7. **Chester, N., F. Kuo, C. Kozak, C. D. O'Hara, and P. Leder.** 1998. Stage-specific apoptosis, developmental delay, and embryonic lethality in mice homozygous for a targeted disruption in the murine Bloom's syndrome gene. Genes Dev. **12**:3382–3393.
8. **Cohen, H., and D. A. Sinclair.** 2001. Recombination-mediated lengthening of terminal telomeric repeats requires the Sgs1 DNA helicase. Proc. Natl. Acad. Sci. USA **98:**3174–3179.
9. **d'Adda di Fagagna, F., P. M. Reaper, L. Clay-Farrace, H. Fiegler, P. Carr, T. Von Zglinicki, G. Saretzki, N. P. Carter, and S. P. Jackson.** 2003. A DNA damage checkpoint response in telomere-initiated senescence. Nature **426:** 194–198.
10. **Ellis, N. A., and J. German.** 1996. Molecular genetics of Bloom's syndrome. Hum. Mol. Genet. **5:**1457–1463.
11. **Ellis, N. A., J. Groden, T. Z. Ye, J. Straughen, D. J. Lennon, S. Ciocci, M. Proytcheva, and J. German.** 1995. The Bloom's syndrome gene product is homologous to RecQ helicases. Cell **83:**655–666.
12. **Epstein, C. J., G. M. Martin, A. L. Schultz, and A. G. Motulsky.** 1966. Werner's syndrome a review of its symptomatology, natural history, pathologic features, genetics and relationship to the natural aging process. Medicine (Baltimore) **45:**177–221.
13. **Forsyth, N. R., W. E. Wright, and J. W. Shay.** 2002. Telomerase and differentiation in multicellular organisms: turn it off, turn it on, and turn it off again. Differentiation **69:**188–197.
14. **Goss, K. H., M. A. Risinger, J. J. Kordich, M. M. Sanz, J. E. Straughen, L. E. Slovek, A. J. Capobianco, J. German, G. P. Boivin, and J. Groden.** 2002. Enhanced tumor formation in mice heterozygous for Blm mutation. Science **297:**2051–2053.
15. **Hande, M. P., E. Samper, P. Lansdorp, and M. A. Blasco.** 1999. Telomere length dynamics and chromosomal instability in cells derived from telomerase null mice. J. Cell Biol. **144:**589–601.
16. **Hasty, P., J. Campisi, J. Hoeijmakers, H. van Steeg, and J. Vijg.** 2003. Aging and genome maintenance: lessons from the mouse? Science **299:**1355–1359.
17. **Herrera, E., E. Samper, J. Martin-Caballero, J. M. Flores, H. W. Lee, and M. A. Blasco.** 1999. Disease states associated with telomerase deficiency appear earlier in mice with short telomeres. EMBO J. **18:**2950–2960.
18. **Hisama, F. M., Y. H. Chen, M. S. Meyn, J. Oshima, and S. M. Weissman.** 2000. WRN or telomerase constructs reverse 4-nitroquinoline 1-oxide sensitivity in transformed Werner syndrome fibroblasts. Cancer Res. **60:**2372–2376.
19. **Huang, P., F. E. Pryde, D. Lester, R. L. Maddison, R. H. Borts, I. D. Hickson, and E. J. Louis.** 2001. SGS1 is required for telomere elongation in the absence of telomerase. Curr. Biol. **11:**125–129.
20. **Huang, S., B. Li, M. D. Gray, J. Oshima, I. S. Mian, and J. Campisi.** 1998. The premature ageing syndrome protein, WRN, is a 3→5′ exonuclease. Nat. Genet. **20:**114–116.
21. **Huber, M. D., D. C. Lee, and N. Maizels.** 2002. G4 DNA unwinding by BLM and Sgs1p: substrate specificity and substrate-specific inhibition. Nucleic Acids Res. **30:**3954–3961.
22. **Imamura, O., K. Fujita, C. Itoh, S. Takeda, Y. Furuichi, and T. Matsumoto.** 2002. Werner and Bloom helicases are involved in DNA repair in a complementary fashion. Oncogene **21:**954–963.
23. **Johnson, F. B., R. A. Marciniak, M. McVey, S. A. Stewart, W. C. Hahn, and L. Guarente.** 2001. The Saccharomyces cerevisiae WRN homolog Sgs1p participates in telomere maintenance in cells lacking telomerase. EMBO J. **20:**905–913.
24. **Kaneko, H., E. Matsui, T. Fukao, K. Kasahara, W. Morimoto, and N. Kondo.** 1999. Expression of the BLM gene in human haematopoietic cells. Clin. Exp. Immunol. **118:**285–289.
25. **Khakhar, R. R., J. A. Cobb, L. Bjergbaek, I. D. Hickson, and S. M. Gasser.** 2003. RecQ helicases: multiple roles in genome maintenance. Trends Cell Biol. **13:**493–501.
26. **Lee, H. W., M. A. Blasco, G. J. Gottlieb, J. W. Horner, 2nd, C. W. Greider, and R. A. DePinho.** 1998. Essential role of mouse telomerase in highly proliferative organs. Nature **392**:569–574.
27. **Liu, J. P.** 1999. Studies of the molecular mechanisms in the regulation of telomerase activity. FASEB J. **13:**2091–2104.
28. **Lombard, D. B.** 2000. Ph.D. thesis. Massachusetts Institute of Technology, Cambridge, Mass.
29. **Lombard, D. B., C. Beard, B. Johnson, R. A. Marciniak, J. Dausman, R. Bronson, J. E. Buhlmann, R. Lipman, R. Curry, A. Sharpe, R. Jaenisch, and L. Guarente.** 2000. Mutations in the *WRN* gene in mice accelerate mortality in a p53-null background. Mol. Cell. Biol. **20:**3286–3291.
30. **Luo, G., I. M. Santoro, L. D. McDaniel, I. Nishijima, M. Mills, H. Youssoufian, H. Vogel, R. A. Schultz, and A. Bradley.** 2000. Cancer predisposition caused by elevated mitotic recombination in Bloom mice. Nat. Genet. **26:** 424–429.
31. **Machwe, A., L. Xiao, and D. K. Orren.** 2004. TRF2 recruits the Werner syndrome (WRN) exonuclease for processing of telomeric DNA. Oncogene **23:**149–156.
32. **McDaniel, L. D., N. Chester, M. Watson, A. D. Borowsky, P. Leder, and R. A. Schultz.** 2003. Chromosome instability and tumor predisposition inversely correlate with BLM protein levels. DNA Repair (Amsterdam) **2:**1387–1404.
33. **Moens, P. B., R. Freire, M. Tarsounas, B. Spyropoulos, and S. P. Jackson.** 2000. Expression and nuclear localization of BLM, a chromosome stability protein mutated in Bloom's syndrome, suggest a role in recombination during meiotic prophase. J. Cell Sci. **113:**663–672.
34. **Monnat, R. J., Jr., and Y. Saintigny.** 2004. Werner syndrome protein-unwinding function to explain disease. Sci. Aging Knowledge Environ. **13:**re3.
35. **Nakayama, H.** 2002. RecQ family helicases: roles as tumor suppressor proteins. Oncogene **21:**9008–9021.
36. **Opresko, P. L., W. H. Cheng, C. Von Kobbe, J. A. Harrigan, and V. A. Bohr.** 2003. Werner syndrome and the function of the Werner protein; what they can teach us about the molecular aging process. Carcinogenesis. **24:**791–802.
37. **Opresko, P. L., C. Von Kobbe, J. P. Laine, J. Harrigan, I. D. Hickson, and V. A. Bohr.** 2002. Telomere-binding protein TRF2 binds to and stimulates the Werner and Bloom syndrome helicases. J. Biol. Chem. **277:**41110–41119.
38. **Orren, D. K., S. Theodore, and A. Machwe.** 2002. The Werner syndrome helicase/exonuclease (WRN) disrupts and degrades D-loops in vitro. Biochemistry **41:**13483–13488.
39. **Parenteau, J., and R. J. Wellinger.** 1999. Accumulation of single-stranded DNA and destabilization of telomeric repeats in yeast mutant strains carrying a deletion of RAD27. Mol. Cell. Biol. **19:**4143–4152.
40. **Parenteau, J., and R. J. Wellinger.** 2002. Differential processing of leading- and lagging-strand ends at Saccharomyces cerevisiae telomeres revealed by the absence of Rad27p nuclease. Genetics **162:**1583–1594.
41. **Parrinello, S., E. Samper, A. Krtolica, J. Goldstein, S. Melov, and J. Campisi.** 2003. Oxygen sensitivity severely limits the replicative lifespan of murine fibroblasts. Nat. Cell Biol. **5:**741–747.
42. **Reddel, R. R.** 2003. Alternative lengthening of telomeres, telomerase, and cancer. Cancer Lett. **194:**155–162.
43. **Rizki, A., and V. Lundblad.** 2001. Defects in mismatch repair promote telomerase-independent proliferation. Nature **411:**713–716.
44. **Rudolph, K. L., S. Chang, H. W. Lee, M. Blasco, G. J. Gottlieb, C. Greider, and R. A. DePinho.** 1999. Longevity, stress response, and cancer in aging telomerase-deficient mice. Cell **96:**701–712.
45. **Schulz, V. P., V. A. Zakian, C. E. Ogburn, J. McKay, A. A. Jarzebowicz, S. D. Edland, and G. M. Martin.** 1996. Accelerated loss of telomeric repeats may not explain accelerated replicative decline of Werner syndrome cells. Hum. Genet. **97:**750–754.
46. **Sharma, S., J. A. Sommers, L. Wu, V. A. Bohr, I. D. Hickson, and R. M. Brosh, Jr.** 2003. Stimulation of flap endonuclease-1 by the Bloom's syndrome protein. J. Biol. Chem. **279:**9847–9856.
47. **Shen, J. C., M. D. Gray, J. Oshima, A. S. Kamath-Loeb, M. Fry, and L. A. Loeb.** 1998. Werner syndrome protein. I. DNA helicase and dna exonuclease reside on the same polypeptide. J. Biol. Chem. **273:**34139–34144.
48. **Stansel, R. M., T. de Lange, and J. D. Griffith.** 2001. T-loop assembly in vitro involves binding of TRF2 near the 3′ telomeric overhang. EMBO J. **20:**5532–5540.
49. **Stavropoulos, D. J., P. S. Bradshaw, X. Li, I. Pasic, K. Truong, M. Ikura, M. Ungrin, and M. S. Meyn.** 2002. The Bloom syndrome helicase BLM interacts

with TRF2 in ALT cells and promotes telomeric DNA synthesis. Hum. Mol. Genet. **11:**3135–3144.
50. **Stein, P., P. Svoboda, D. J. Stumpo, P. J. Blackshear, D. B. Lombard, B. Johnson, and R. M. Schultz.** 2002. Analysis of the role of RecQ helicases in RNAi in mammals. Biochem. Biophys. Res. Commun. **291:**1119–1122.
51. **Takai, H., A. Smogorzewska, and T. de Lange.** 2003. DNA damage foci at dysfunctional telomeres. Curr. Biol. **13:**1549–1556.
52. **Tarsounas, M., P. Munoz, A. Claas, P. G. Smiraldo, D. L. Pittman, M. A. Blasco, and S. C. West.** 2004. Telomere maintenance requires the RAD51D recombination/repair protein. Cell **117:**337–347.
53. **Tyner, S. D., S. Venkatachalam, J. Choi, S. Jones, N. Ghebranious, H. Igelmann, X. Lu, G. Soron, B. Cooper, C. Brayton, S. Hee Park, T. Thompson, G. Karsenty, A. Bradley, and L. A. Donehower.** 2002. p53 mutant mice that display early ageing-associated phenotypes. Nature **415:**45–53.
54. **Von Zglinicki, T.** 2003. Replicative senescence and the art of counting. Exp. Gerontol. **38:**1259–1264.
55. **Watt, P. M., I. D. Hickson, R. H. Borts, and E. J. Louis.** 1996. SGS1, a homologue of the Bloom's and Werner's syndrome genes, is required for maintenance of genome stability in Saccharomyces cerevisiae. Genetics **144:** 935–945.
55a. **Wang, K. K., S. Chang, S. R. Weiler, S. Ganesan, J. Chandhuri, C. Zhu, S. E. Artandi, K. L. Rudolph, G. J. Gottlieb, L. Chino, F. W. Alt, and R. A. DePinho.** 2000. Telomere dysfunction impairs DNA repair and enhances sensitivity to ionizing radiation. Nat. Genet. **26:**85–88.
56. **Wong, K. K., R. S. Maser, R. M. Bachoo, J. Menon, D. R. Carrasco, Y. Gu, F. W. Alt, and R. A. DePinho.** 2003. Telomere dysfunction and Atm deficiency compromises organ homeostasis and accelerates ageing. Nature **421:** 643–648.
57. **Wright, W. E., M. A. Piatyszek, W. E. Rainey, W. Byrd, and J. W. Shay.** 1996. Telomerase activity in human germline and embryonic tissues and cells. Dev. Genet. **18:**173–179.
58. **Wyllie, F. S., C. J. Jones, J. W. Skinner, M. F. Haughton, C. Wallis, D. Wynford-Thomas, R. G. Faragher, and D. Kipling.** 2000. Telomerase prevents the accelerated cell ageing of Werner syndrome fibroblasts. Nat. Genet. **24:**16–17.
59. **Yankiwski, V., R. A. Marciniak, L. Guarente, and N. F. Neff.** 2000. Nuclear structure in normal and Bloom syndrome cells. Proc. Natl. Acad. Sci. USA **97:**5214–5219.
60. **Yu, C. E., J. Oshima, Y. H. Fu, E. M. Wijsman, F. Hisama, R. Alisch, S. Matthews, J. Nakura, T. Miki, S. Ouais, G. M. Martin, J. Mulligan, and G. D. Schellenberg.** 1996. Positional cloning of the Werner's syndrome gene. Science **272:**258–262.